

JAAS

Accepted Manuscript



This is an *Accepted Manuscript*, which has been through the Royal Society of Chemistry peer review process and has been accepted for publication.

Accepted Manuscripts are published online shortly after acceptance, before technical editing, formatting and proof reading. Using this free service, authors can make their results available to the community, in citable form, before we publish the edited article. We will replace this *Accepted Manuscript* with the edited and formatted *Advance Article* as soon as it is available.

You can find more information about *Accepted Manuscripts* in the [Information for Authors](#).

Please note that technical editing may introduce minor changes to the text and/or graphics, which may alter content. The journal's standard [Terms & Conditions](#) and the [Ethical guidelines](#) still apply. In no event shall the Royal Society of Chemistry be held responsible for any errors or omissions in this *Accepted Manuscript* or any consequences arising from the use of any information it contains.

1
2
3 **Quantitative evaluation on ante-mortem lead in human remains of the 18th**
4 **century by triaxial geometry and bench top micro X-ray fluorescence**
5 **spectrometry**
6

7 A. A. Dias¹, M. Carvalho¹, M. L. Carvalho¹ and S. Pessanha^{1*}
8

9
10 ¹LIBPhys-UNL, Laboratory for Instrumentation, Biomedical Engineering and Radiation
11 Physics, and Departamento de Física da Faculdade de Ciências e Tecnologia,
12 Universidade Nova de Lisboa, 2829-516 Caparica
13

14 *Corresponding author: sofia.pessanha@fct.unl.pt
15

16 **Abstract**
17

18 The aim of this work is to demonstrate the suitability of the commercial benchtop
19 micro X-ray fluorescence (μ -XRF) system M4 Tornado, to evaluate the differences on
20 lead distribution in the different bone and tooth structures. *Ante-mortem* and *post-*
21 *mortem* Pb accumulation was also assessed and the lead amount in the different tissues
22 was compared. Micro-XRF based in polycapillary systems is a relatively new technique
23 with capabilities to provide multielemental maps and quantitative measurements.
24 Another advantage of the technique is being non-destructive and requiring only a small
25 amount of sample.
26

27 In this work we measured the lead concentration in human remains, bone and tooth of
28 an 18th century young male subject, around 30 years old, and compared the results
29 obtained using the μ -XRF with a setup with triaxial geometry. Accuracy of the
30 microanalytical system for pressed pellets and cross sections of bone and tooth were
31 also certified.
32

33 The μ -XRF setup provided analytical point spectra, line profiles and elemental maps for
34 Pb and Ca distribution in bone and tooth. The quantitative calculations were accessed
35 by the fundamental parameters and compared mode methods. The accuracy and the
36 detection limits were checked using standard reference materials for Ca, Zn, Sr and Pb.
37 Furthermore, unusual extremely high amounts of Pb in cortical bone, tibia and fibula,
38 were observed, reaching $120 \pm 10 \mu\text{g.g}^{-1}$, while the trabecular region reached 250 ± 20
39 $\mu\text{g.g}^{-1}$. Rib presented the highest levels, $560 \pm 30 \mu\text{g.g}^{-1}$. In tooth structure the highest
40 amount of Pb was found in pulp and root with $130 \pm 50 \mu\text{g.g}^{-1}$. Low levels of Pb in the
41 surrounding soil have been found.
42
43
44
45
46
47
48
49
50
51
52
53
54
55
56
57
58
59
60

Keywords: Lead concentration; human bone; micro-X ray fluorescence; triaxial geometry; tooth;

1. Introduction

X ray fluorescence technique is known to be a powerful technique for measurement of trace elements in a variety of solid matrices, including biological and environmental samples¹⁻⁵. In the past 20 years much research has been done measuring trace elements and elemental constitution of human bone, many of them using X-ray Fluorescence. Spatial distribution of trace elements at the micrometer scale, were obtained in bone, by a benchtop monochromatic microbeam X-ray fluorescence setup⁶. PIXE and nuclear microprobe were also used for elemental distribution⁷⁻¹⁰. The concentration of lead in tibia (cortical bone) and calcaneus (trabecular bone) was measured by an *in vivo* X-ray fluorescence technique in active contemporary workers with a system based on the non-invasive ¹⁰⁹Cd excited K X-ray fluorescence technique¹¹⁻¹⁴. Chemical analyses and atomic absorption spectroscopy allow measurement of the elemental concentration, but they have the disadvantage of being destructive¹⁵. Lead concentrations in several cortical and trabecular bones in deceased smelter workers has been obtained by electrothermal atomic absorption spectrometry¹⁶. Laser ablation inductively coupled plasma mass spectrometry has also been used for quantitative measurements of lead in bone¹⁷. Electron probe micro analyses offer a spatial resolution in the micrometer and sub-micrometer range, but suffer from low sensitivity for some elements such as Sr, U, Ba, Zn and Pb, which are often present in fossilized bone^{18, 19}.

PIXE and X-ray micro fluorescence analyses are both multielemental, non-destructive and the detection limits are at the μg level. The spatial resolution reachable depends on the experimental set-up and is in the range of μm^2 to several mm^2 . Synchrotron microprobe has also been used in bone analysis²⁰.

A potentially important and little explored application of micro X-ray fluorescence (μXRF) is the measurement of the spatial elemental distribution in forensic applications, namely the elemental distribution of lead or other toxic metals in gunshot residues^{21,22}. Such studies are required to develop and understanding the biological fate of ingested heavy metals or poisoning compounds following environmental or occupational exposure, or following deliberate administration during drug therapy. In the case of lead, this data would be valuable for the application of bone lead measurements as a biomarker and determining Pb long-term ingestion or acute intoxications. Whilst

1
2
3 qualitative or semi-quantitative data are sufficient for some applications, rigorous
4 quantitative analysis is desirable for clinical, biomedical and forensic samples²³.

5
6 Bone and tooth are the hardest structures of the human body. Both have been considered
7 good biomarkers for man elemental exposure being the main targets for the deposition
8 of heavy metals, and good indicators for long range exposure. Bone consists of cortical
9 (substantia compacta) as well as trabecular bone (substantia spongiosa). The high
10 porosity of the spongy bone and its open morphology makes it more susceptible to *post-*
11 *mortem* alteration^{24, 25}. Tooth consists of three main components: enamel, dentine and
12 pulp. In human remains, lead can be both from *post-mortem* and *antemortem* origin.
13 Inner compact tissue might represent in vivo accumulation and trabecular one
14 corresponds to uptake during burial. Physical and chemical changes can occur in bone
15 during its burial period. As bone is fossilized, the natural process of diagenesis serves to
16 alter the bone composition from its *ante-mortem* state. These processes and their rate of
17 reaction mainly depend on direct environmental conditions such as groundwater, soil
18 composition, soil pH, redox potential and temperature.

19
20 In this work the spatially resolved elemental analysis in human remains, bone and tooth
21 has been achieved by the micro-analytical commercial M4 Tornado (Bruker) with
22 capability for elemental distribution at a spatial resolution of 25 μm . This is a benchtop
23 nondestructive method and the quantification process is easy to handle with appropriate
24 calibration. The quantitative calculations were checked by a second equipment with
25 triaxial geometry and very well documented for many kinds of samples²⁻⁵. The results
26 obtained with the two systems in terms of Pb *antemortem* accumulation from
27 environmental exposure during life and *post-mortem* uptake from the burial place, are
28 discussed and explored through the distribution patterns of Pb along the tooth, and bone.
29 The obtained values show strongly increased levels of lead especially in spongy bone.
30 However, the compact bone also showed unusually high values for this element, which
31 may indicate *ante-mortem* Pb-exposure. Furthermore, in the tooth, the highest values of
32 Pb were found in the pulp and root, confirming *ante-mortem* Pb-exposure, considering
33 that low levels of Pb in soil were found.

34 35 36 37 38 39 40 41 42 43 44 45 46 47 48 49 50 51 52 53 54 **2. Experimental**

55 56 **2.1. Sample collection and preparation**

57
58
59
60

1
2
3 In this work we report the analysis of several bones and teeth of one particular subject,
4 who was part of a collection of 83 individuals recovered from the inside of a chapel,
5 dating from 18th-19th centuries²⁶. This was a young male, around 30 years old, laying
6 about 1 m deep. The bone material consisted of several ribs, foot bone, thighs, skull,
7 femur, fibula and tibia both compact and trabecular bones. Several teeth were also
8 collected. In order to evaluate possible contaminations from the burial surroundings, we
9 also analyzed the soil.

10
11
12 Each bone and tooth were rinsed in tap water and carefully brushed, to remove
13 completely the soil. After this cleaning process the samples were washed in distilled
14 water, dried in a clean environment at room temperature.

15
16
17 From each bone a few grams from the inner compact and trabecular area bone were
18 taken, by means of a polyester tool. Prior to analysis each sample was powdered in a
19 polyester mill and the obtained fine powder was pressed into pellets 1.5 cm in diameter
20 and 1 mm thick, without any chemical treatment. A minimum of three pellets of each
21 sample, and a minimum of 3 samples of each type were taken to minimize the effects of
22 inhomogeneity. Each pellet was glued on a Mylar film, on a sample holder and placed
23 directly under the X-ray beam, for elemental determination, as described in Guimarães
24 et al³.

25
26
27 During the grinding sample preparation, special care has been paid to contamination, as
28 well as during the whole procedure. All the material used is made of polyester, to avoid
29 any contact with metals. For microanalysis, transversal sections of femur and
30 longitudinal slices of tooth, around 1mm thick, were obtained with a microtome
31 equipped with a diamond saw and the samples were placed directly on the x-ray
32 microbeam.

33 34 35 36 37 38 39 40 41 42 43 44 45 **2.2. Experimental setup**

46 47 48 **2.2.1. Benchtop microanalytical system**

49 In this work we used a commercial benchtop spectrometer, the M4 Tornado by Bruker
50 (Germany) for elemental mapping. The X-ray tube is a micro-focus side window Rh
51 tube powered by a low power HV-generator and cooled by air. A poly-capillary lens is
52 used to obtain a spot size down to 25 μm for Mo-K α . The X-ray generator was operated
53 at 50 kV and 300 μA and a composition of filters was used to reduce the background
54 (100 μm Al/ 50 μm Ti/ 25 μm Cu). Under these conditions we could almost eliminate
55
56
57
58
59
60

1
2
3 the energy radiation below 9 keV of the bremsstrahlung. This, together with the
4 preferential reflexion energy for the poly-capillary, the experimental setup allows a
5 quasi-monochromatic beam between 9-15 keV, much better than the white incident
6 beam originated from the X-ray tube. The detection of the fluorescence radiation is
7 performed using a thermoelectrically cooled Silicon-Drift-Detector with energy
8 resolution of 142 eV for Mn-K α .
9

10
11 Measurements were carried out under 20 mbar vacuum conditions. The vacuum system
12 avoids back diffusion and improves detection limits. This equipment was used to
13 perform mappings of cross sections of the bones and tooth samples. Spectra
14 deconvolution and fitting were performed using WinAXIL software package (Canberra,
15 Belgium) and quantification was performed through compare mode²⁷. This method
16 makes use of SRM with the same matrix and similar elemental composition as the
17 unknown sample to determine the sensitivity for each element and configure the
18 quantification procedure.
19
20
21
22
23
24
25
26

27 **2.2.2. Triaxial geometry**

28
29 One of the used spectrometers to quantify Pb in bone consists of a high power X-ray
30 tube with a tungsten anode, water cooled, equipped with a changeable secondary target
31 of molybdenum. This arrangement makes it possible to obtain a monochromatic source
32 and to select the secondary target in order to get the best excitation conditions for a
33 special element. The X-ray tube, the secondary target and the sample are in a triaxial
34 geometry. With this arrangement we decrease the background, taking the advantage of
35 the effect of the partial polarization of the incident x-ray beam from the tube, and so
36 improving the detection limits²⁸. The characteristic radiation emitted by the elements
37 present in the sample was detected by a Si(Li) detector, with a 30 mm² active area and 8
38 μ m beryllium window. The energy resolution is 135 eV at 5.9 keV and the acquisition
39 system is a Nucleus PCA card. The X-ray generator was operated at 50 kV and 20 mA
40 and a typical acquisition time of 1000 s was used. The beam size on the sample is
41 around 1.5 cm x 2.0 cm. Quantitative calculations are made through the fundamental
42 parameters method. Experimental parameters were obtained through calibration, using
43 standard reference bone materials.
44
45
46
47
48
49
50
51
52
53
54

55 **3. Accuracy tests**

56 **3.1. Pressed pellets**

1
2
3 The accuracy of the benchtop microanalytical system has been checked by analyzing
4 pressed pellets of, SRM NIST-1400 bone ash ($9.1 \mu\text{g g}^{-1}$ of Pb), NYS RM 05-02 bovine
5 bone ($16.1 \mu\text{g g}^{-1}$ of Pb) and NYS RM 05-04 caprine bone ($31.5 \mu\text{g g}^{-1}$ of Pb) pellets
6 and the values are presented in Table 1. The detection limits were also obtained and are
7 presented in the same table. As one of the main goals of this work is to study the
8 performance of this microanalytical system for Pb evaluation, we checked other bone
9 reference materials with lower amount of Pb, NYS RM 05-01, bovine bone with 1.09
10 $\mu\text{g g}^{-1}$ and NIST SRM 1486, bone meal, with an amount of Pb $1.4 \mu\text{g g}^{-1}$. It was not
11 possible to detect Pb for the first material and for the second one it was impossible to
12 quantify. Considering that this technique is multielemental, besides Pb, the accuracy
13 and the detection limits have been also evaluated for Ca, Zn and Sr, elements of
14 foremost importance for their relationship to Pb²⁹. Burial soil has also been analyzed
15 and the accuracy of the system for this complicated matrix has also been checked by
16 SRM IAEA-soil 7. The results are presented in Table 2.

17
18 The accuracy of the triaxial geometry system for bone samples was checked by analysis
19 of two pressed pallets of standard reference materials; caprine bone NYS RM 05-04 and
20 caprine bone NYS RM 05-02, with 30 and $16 \mu\text{g g}^{-1}$ Pb concentration respectively. The
21 accuracy and detection limits were also calculated and the results are presented in Table
22 1.

23
24 Considering that the amount of Pb in the present bone samples was much higher than
25 the one in the reference material, the accuracy of the systems for such high values
26 needed further requirement. Taking into account the lack of such certified reference
27 materials in the market, another bone sample previously analyzed has been used as
28 reference. In a previous work², bone samples have been studied by ¹⁰⁹Cd-based X-ray
29 fluorescence. Pressed pellet samples with an amount of Pb of $330 \mu\text{g g}^{-1}$ have been
30 used. Together with these pellets, reference calibrated phantoms of plaster of Paris
31 reference material with ($200 \mu\text{g Pb/g}$ bone mineral) have also been used.

3.2. Mapping

32
33 Transversal cross-sections from the tibia and longitudinal cross-sections from the teeth
34 were cut by a microtome with a diamond saw, 1 mm thick. Each sample was mounted
35 directly on a table 360 mm x 260 mm, which was attached to a stage translatable along
36
37
38
39
40
41
42
43
44
45
46
47
48
49
50
51
52
53
54
55
56
57
58
59
60

1
2
3 XY, and analysed directly by μ XRF. The scanning step size was 25 μ m. For each point,
4 the counting time was 3.76 s.

5
6 Each sample was analyzed over a period of 12 h, to accumulate sufficient data points for
7 high resolution mapping. The analysis was fully automated and unattended. The
8 counting time and the scanning spatial resolution are freely selected according to the
9 required resolution. A CCD camera allows visualize the studied area. The data output
10 was arranged into a table giving the X-ray intensity of specific X-ray peaks representing
11 element signals each measured point defined by its X and Y coordinate (μ m).

12
13 The data were converted using the software's function into a data matrix, from which
14 XY contour maps (2-dimensional maps) of the data were generated for each element. In
15 Fig. 1 and 2 the elemental maps for Pb and Ca both in tibia and tooth cross section
16 respectively, are presented.

23 24 25 **4. Results and Discussion**

26 27 **4.1. Quantification on pressed pellets**

28
29 From the results presented in Tables 1 and 2 for accuracy in bone and soil pressed pellet
30 samples we can conclude that very good agreement is obtained with the microanalytical
31 equipment. From Table 1 we also conclude that good agreement between reference
32 bone material and the values obtained with the triaxial system is observed. Furthermore,
33 when we compare the results obtained by the microanalytical system, with the obtained
34 by the triaxial one, the most important finding is that the uncertainty of the obtained
35 values is higher in the microanalytical system. In Fig. 3 we display one spectrum of a
36 bone obtained with both setups, to better evidence the background obtained by the two
37 systems. There is a reduction on the scattered radiation in the microanalysis system in
38 the interest region and especially on the low energy side, with the vanishing of the Ar
39 from the air, due to vacuum conditions. This is essential when light elements are
40 important like P in tooth. Moreover, the use of the polycapillary also contributes to
41 improve the background to peak ratio.

42
43 The elemental distribution Ca and Pb can be observed in Fig. 1 for tooth longitudinal
44 cross section and in Fig. 2 for tibia transversal cut, respectively for Ca and Pb. Calcium
45 is more or less uniformly distributed in both samples, Pb appeared to be enriched in the
46 inner part of the tooth, pulp and root. Concerning bone samples an increase of Pb is
47
48
49
50
51
52
53
54
55
56
57
58
59
60

1
2
3 visible on the outer surface. In the inner spongy bone we distinguish small spots with
4 enhanced level of Pb.
5

6 From the literature we can find studies devoted to assess *post-mortem* Pb in bones
7 buried in contaminated environments and on the other side we can find research works
8 dedicated to the *ante-mortem* Pb distribution and quantification. In this case we can find
9 studies obtained either by *in vivo* analysis or from autopsy of deceased people.
10

11 Buried bones in contaminated environments were studied by M. L. Carvalho^{1,2,30} in
12 contaminated soils and a lead coffin by X-ray fluorescence based techniques. Femoral
13 sections of a woman skeleton buried in lead sarcophagus were also studied¹⁰. Another
14 important study on Pb uptake from the burial soil was the study of a mining population
15 buried in a very high Pb contaminated soil close to the mining area⁹. In all studies the
16 levels of Pb in the outer parts of the bone or in the trabecular regions were tremendously
17 increased evidencing strong *post-mortem* enrichment of Pb. The highest concentrations
18 correspond to large pores and voids in the bone structure, while compact tissue with
19 harder structure is less susceptible to Pb uptake. The exchange mechanisms between the
20 archaeological bone and its neighborhood were obvious. The concentration profiles
21 obtained from the outside of the bone to the inner part confirm that Pb penetrated into
22 the bone matrix. The diffusion of the metal was from the outside to the inner structure
23 of the compact bone, which remained almost non-affected. The ratios between
24 concentration values in the different structures reached one to several orders of
25 magnitude, depending on the degree of contamination of the mortuary environment. The
26 amount of Pb deeply decreased from the affected areas to the inner compact bone
27 showing that the Pb in bones was obtained by *post-mortem* uptake.
28

29 Concerning *ante-mortem* Pb distribution it can be obtained either by *in vivo* analysis or
30 from autopsy in deceased people. The most relevant work on *in vivo* analysis can be
31 found in a summarized work by D. Chettle¹⁴. Furthermore three works on deceased
32 people deserve to be referred^{8, 16, 29}. U. Lindh⁸ carried out by micro-PIXE with a spatial
33 resolution of 5 μm , the analysis of two human femurs; one belonged to a worker
34 exposed to lead in heavy metal industry, and the other worker was from the same
35 environment but not exposed to lead. The mean lead concentration in the poisoned and
36 the reference case in compact bone was 70 and 30 $\mu\text{g g}^{-1}$, respectively. The poisoned
37 case exhibited two peaks in the distribution, at distances of approximately 0.2 and 1.8
38 mm from the periphery, respectively.
39
40
41
42
43
44
45
46
47
48
49
50
51
52
53
54
55
56
57
58
59
60

1
2
3 The work of L. Gerhardsson¹⁶ aimed to compare bone lead concentrations in several
4 cortical and trabecular structures in long-term exposed lead smelter workers, and to
5 relate the measured concentrations to the corresponding ones in non-exposed workers.
6 He analyzed, by electrothermal AAS, seven bones (trabecular: sternum, vertebrae, iliac
7 crest, rib; cortical: femur, forefinger, and temporal bone) in 32 male, long-term exposed
8 to lead and 10 non-unexposed male, reference persons. Furthermore this study presents
9 values for Sr and Zn in the same bones. Todd²⁹ studied by electrothermal AAS adult
10 human tibia for lead concentration determination. The goal of this work was to
11 determine whether there were any differences between core and surface tibia lead
12 concentrations. Lead concentrations in the nine tibiae ranged from 3.1 to 27.9 µg lead/g
13 of dry bone. They concluded that the studied human tibiae showed a greater surface
14 tibia lead concentration than core tibia lead concentration by a factor of the order of 2.
15

16 The indication of preferential accumulation in trabecular (spongy) rather than cortical
17 bone by a factor around 1.4 in contaminated people was observed by Gerhardsson¹⁶. A
18 factor of 2 has been observed by Chettle¹⁴ by in vivo analysis of calcaneus and tibia.
19

20 In the present work the concentration values obtained in pressed pellets for the several
21 bones are presented in tables 3 and 4 respectively for M4 Tornado and triaxial system
22 for Ca, Zn, Sr and Pb. The agreement between the results obtained with both systems is
23 remarkable. However, as already noticed for accuracy authentication, the uncertainties
24 are higher for microanalytical system, of the order of 20% while for the triaxial system
25 the uncertainty is around 10%. Nevertheless, from these values we can deduce that
26 quantification for the benchtop microanalytical system with reasonable accuracy for Ca,
27 Zn, Sr and Pb in pressed pellets is possible. The highest values for Pb were found in
28 spongy bones: ribs, followed by the skull, foot bone, femur, fibula and tibia. Finally the
29 inner part of thick compact bones, fibula and tibia present the lowest concentrations.
30 The ratio between the content of Pb in both spongy and compact area of the same bone
31 is around 2.
32

33 The relation between the amount of Pb in these bones is similar with the one obtained
34 by Gerhardsson¹⁶ in workers exposed to Pb contamination for around 30 years.
35 However the values obtained in the present work are much higher than the mean values
36 in that work. In Fig. 4 we can compare a spectrum from soil and compact bone. It is
37 obvious that Pb in soil is much lower than in bone. From this result and considering that
38 the ratio Pb content in spongy and compact bone is of the order of 2 we can deduce that
39 the subject under study was *ante-mortem* contaminated.
40
41
42
43
44
45
46
47
48
49
50
51
52
53
54
55
56
57
58
59
60

1
2
3 Concerning the values of Sr they are more or less constant in all the studied bones, as
4 well as the levels of Ca. Unlikely, Zn presents high variation in the different bones.
5
6
7

8 **4.2. Quantification in microanalysis elemental distribution**

9
10 For complete calibration of the benchtop system it is necessary to guarantee that
11 quantification directly on the samples, without any sample preparation, is possible and
12 accurate. This is actually the main goal of this study. To accomplish this purpose we
13 used the slices of tibia bone and tooth and carried out quantitative calculations on
14 several points. The results obtained for tibia are displayed in Fig. 5. They are in very
15 good agreement with the corresponding ones obtained in pressed pellets. The lowest
16 concentration values are obtained in the inner part of the tibia compact bone and
17 enriched levels are observed on the direction of the spongy bone. A tendency to
18 accumulation in the outer surface is also evident, in agreement with the results observed
19 in the distribution mapping. Furthermore we also could confirm a factor of 2 for the
20 ratio between the minimum and maximum value, in agreement with the attained values
21 in pressed pellets. Determination on the micro distribution of Sr and Pb have been
22 carried out by Bellis⁶ using a prototype benchtop XRF system based on focused
23 monochromatic microbeam X-ray fluorescence with a low power source coupled to
24 doubly curved crystal (DCC) optics. However in this work the authors do not performed
25 quantitative calculations. Only elemental maps have been obtained. Elemental
26 distribution is not enough in most cases, as referred, and quantitative analysis is crucial.
27 The conclusions of the present work are however similar to those obtained by Bellis.
28 Lead appeared to accumulate in a thin band near the periosteal surface. Elevation in
29 scattered discrete spots was also observed at the endosteal surface, and to a lesser extent
30 within the core, also in agreement to the findings of Todd²⁹, who found that Pb
31 measurements performed on human tibiae showed that Pb was enriched at the tibia
32 surface relative to the core and that lead concentrations were significantly lower toward
33 the ends of the tibia sections.
34
35
36
37
38
39
40
41
42
43
44
45
46
47
48
49

50 For tooth quantitative elemental micro analytical calculations we obtained the values for
51 P, Ca, Zn, Sr and Pb. The values are presented on table 5. Two different parts can be
52 considered; the pulp and the hard enamel, dentine and root. Pulp presents a completely
53 different matrix in what concerns P, Ca, Sr and Zn, although presenting the highest
54 values for Pb accumulation. This pattern is in agreement with lead *ante mortem*
55
56
57
58
59
60

1
2
3 intoxication³¹⁻³³. Lead circulates in very high concentrations in blood of intoxicated
4 people and might accumulate preferably in pulp region highly irrigated. Phosphorus
5 and Ca are more or less constant in enamel, dentine and root. Zinc is enriched in root
6 following the behavior of Sr and Pb.
7
8
9

10 11 12 13 **5. Conclusions**

14 From this work we could conclude that micro X-ray analytical technique based on a
15 polycapillary system is a powerful technique for Pb determination in hard and soft
16 tissues at the level of 3 $\mu\text{g g}^{-1}$ with 20% uncertainty. Furthermore we also demonstrate
17 the capabilities for elemental distribution with micrometer resolution and quantitative
18 calculations for other elements of biological interest, like P, Ca, Zn and Sr. These are
19 obvious advantages when comparing this system to other XRF based techniques, like
20 synchrotron radiation. Furthermore, the other benefits of the system, being non-
21 destructive and very low amount of sample being necessary make it the preferred choice
22 instead of AAS, ICPMS, LA-ICP-MS when non-destructive process is required. In
23 addition, our results indicate a tendency of higher accumulation of lead in spongy
24 bones. Finally the inner part of thick compact bones, fibula and tibia present the lowest
25 concentrations. The ratio between the content of Pb in both spongy and compact area of
26 the same bone is around 2. This was the ratio found by Chettle¹⁴ when analyzing the
27 bones of exposed individuals. The ratio of Pb in buried bones in contaminated
28 environment is much higher, from 1 to several orders of magnitude^{1, 2, 9, 10}. Moreover,
29 to support the *ante-mortem* contamination explanation, we believe that it is unlikely that
30 a soil about 50 $\mu\text{g.g}^{-1}$ of Pb³⁴ was the cause for contamination. We were dealing with a
31 case of severe lead poisoning of a rather young man. An important source of Pb intake
32 might have been linked to smelter exposure. In addition, the properties of lead, its
33 corrosion resistance and formability, made it extensively used in plumbing, building,
34 and ship construction existing in the area.
35
36
37
38
39
40
41
42
43
44
45
46
47
48
49
50

51 52 53 **Acknowledgements**

54 Authors would like to thank Almada Municipality, namely archaeologist Fernando
55 Henriques Robles and anthropologist Francisco Curate for supporting the investigation.
56
57
58
59
60

1
2
3 S. Pessanha acknowledges Portuguese Fundação para Ciência e Tecnologia for the post-
4 doc grant SFRH/BPD/94234/2013.
5
6
7
8
9
10
11
12
13
14
15
16
17
18
19
20
21
22
23
24
25
26
27
28
29
30
31
32
33
34
35
36
37
38
39
40
41
42
43
44
45
46
47
48
49
50
51
52
53
54
55
56
57
58
59
60

References.

A. Name, B. Name and C. Name, *Journal Title*, year, **volume**, page

1. M.L. Carvalho, A.F. Marques, M.T. Lima, U. Reus, *Spectrochim. Acta B At. Spectrosc*, 2004, **59**, 1251–1257.
2. J. Rebôcho, M. L. Carvalho, A.F. Marques, F. R. Ferreira, and D. R. Chettle, *Talanta*, 2006, **70**, 957–961.
3. D. Guimarães, M. L. Carvalho, V. Geraldés, I. Rocha, and J. P. Santos, *Metallomics*, 2012, **4**, 66–71
4. E. Margui, A. F. Marques, M. L. Prisal, I. Queralt, M. Hidalgo and M. L. Carvalho, *Appl Spectrosc*, 2014, **68**, 1241-1246
5. O. Gonzalez-Fernandez, M. J. Batista, M.M. Abreu, I. Queralt, M.L. Carvalho, *X-Ray Spectrom*, 2011, **40**, 353-363
6. D. J. Bellis, D. Li, Z. Chen, W. M. Gibson, and P. J. Parsons, *J. Anal. At. Spectrom*, 2009, **24**, 622–626
7. T.A. Elliott, G.W. Grime, *Nucl. Instr. Meth. B*, 1993, **77**, 537.
8. U. Lindh, G. Nordberg, and D. Brune, *Sci of the Total Environm*, 1978, **10**, 31-37
9. R. Brenn, Ch. Haug, U. Klar, S. Zander, K.W. Alt, D.N. Jamieson, K.K. Lee and H. Schutkowski, *Nucl Inst and Meth B*, 1999, **158**, 270-274
10. N. Boscher-Barre, P. Trocellier, *Nucl. Instr. Meth. B*. 1993, **73**, 413.
11. C. L. Gordon, D. R. Chettle and C.E. Webber, *British J. of Indust Med*, 1993, **50**, 637-641
12. J. A. A. de Brito, M L Carvalho and D R Chettle, *Phys Med Bio*, 2009, **54**, 919-934
13. J. Brito, F. E. McNeill, C. E. Webber, S. Wells, N. Richard, M. L. Carvalho and D. R. Chettle, *J Environ Monit*, 2002, **4**, 194-201
14. D.Chettle, *X-ray Spectrom*. 2005, **34**, 446–450.
15. Jr. L. Wittmers, A.C. Aufderheide, J.G. Pounds, K.W. Jones, and J.L. Angel, *Am. J. Phys Anthropol*, 2008, **136**, 379–386
16. L. Gerhardsson, A. Akantis, N. G. Lundström, G. F. Nordberg, A. Schütz, and S. Skerfving, *J. Trace Elem. Med. Bio.*, 2005, **19**, 209–215
17. D. J. Bellis, K. M. Hetter, J. Jones, D. Amarasiriwardena and P. J. Parsons, *J. Anal. At. Spectrom*, 2006, **21**, 948–954
18. J.B. Lambert, S.V. Simpson, J.E. Buikstra and D. Hanson, *Am. J. Physical Anthropology*, 1983, **62**, 409-413.

- 1
2
3 19. J.B. Lambert, L. Xue and J.E. Buikstra, *J. Archaeol. Sci.*, 1991, **18**, 363-367.
4 20. N. Zoeger, P. Wobrauschek, C. Strel, G. Pepponi, P. Roschger, G. Falkenberg,
5 and W. Osterode, *X Ray Spectrom*, 2005, **34**, 140–143
6
7 21. J. F. Fonseca, M. M. Cruz and M. L. Carvalho, *X-Ray Spectrom*, 2011, **443**, 49–55
8
9 22. M. López-López, M. Á. Fernández de la Ossa, and C. García-Ruiz, *Appl. Spectrosc.*,
10 2015, **69**, 889-893
11
12 23. J. Kawai, *X Ray Spectrom*, 2014, **43**, 2–12
13
14 24. M. L. Carvalho, C. Casaca, T. Pinheiro, J. P. Marques, P. Chevallier, and A. S.
15 Cunha, *Nucl. Inst Meth B*. 2000, **168**, 559–565.
16
17 25. M.L. Carvalho, A. F. Marques, J.P. Marques, C. Casaca, *Spectrochim. Acta B*. 2007,
18 **62**, 702–706.
19
20 26. F. T. Curate, S. F. R. Henriques, V. Matos, A. Tavares in *Mortalidade Infantil*
21 *na Ermida do Espírito Santo (Almada): entre o afecto e a marginalização*, Al-Madan,
22 Lisboa, 2015, **19**, 68–76.
23
24 27. M. Manso, S. Pessanha, F. Figueira, S. Valadas, A. Guilherme, M. Afonso, A.C.
25 Rocha, M.J. Oliveira, I. Ribeiro, M.L. Carvalho, *Anal. Bioanal. Chem*, 2009, **395**, 2029-
26 2036.
27
28 28. S. Pessanha, A. Guilherme, M.L. Carvalho, *Appl Phys A*, 2009, **97**, 497–505
29
30 29. A.C. Todd, P.J. Parsons, S. Tang, E.L. Moshier, *Environ. Health. Perspect.* 2001,
31 **109**, 1139–1143.
32
33 30. M. L. Carvalho and A. F. Marques, *X Ray Spectrom*, 2008, **36**, 32-36
34
35 31. A.F. Marques, J.P. Marques, C. Casaca and M.L. Carvalho, *Spectrochim Acta B*,
36 2004, **59**, 1675-1680
37
38 32. M. L. Carvalho, J. P. Marques, A. F. Marques, and C. Casaca, *Spectrochim. Acta B*,
39 2007, **62**, 702-706
40
41 33. T. Pinheiro, M. L. Carvalho, C. Casaca, M. A. Barreiros, A. S. Cunha and P.
42 Chevallier, *Nucl. Inst. and Meth B*, 1999, **158**, 393-398
43
44 34. S. Pessanha, M. Carvalho, M.L. Carvalho, A.A. Dias, *J tr elem med biol*,
45 <http://dx.doi.org/10.1016/j.jtemb.2015.08.004>
46
47
48
49
50
51
52
53
54
55
56
57
58
59
60

Figure captions

Fig. 1. Calcium and Pb mappings obtained using the microanalytical system on a tooth longitudinal cross-section

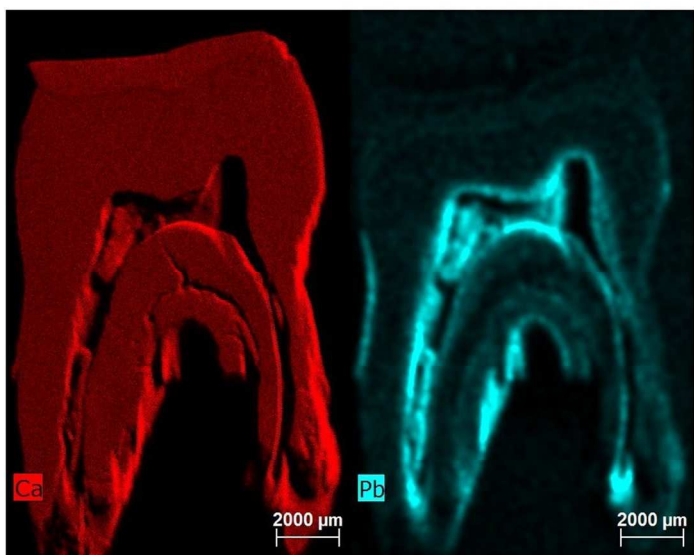
Fig. 2. Calcium and Pb mappings obtained using the microanalytical system on a tibia transversal cross-section

Fig. 3. Bone spectra obtained using both microanalytical and triaxial systems

Fig. 4. Comparison of the spectra obtained for soil and compact bone samples

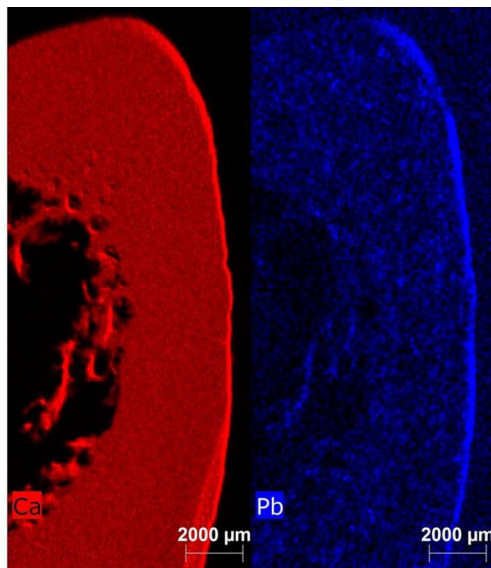
Fig. 5. Lead distribution along a slice of tibia bone obtained using the M4 Tornado from the external part to the inner bone.

1
2
3
4
5
6
7
8
9
10
11
12
13
14
15
16
17
18
19
20
21
22
23
24
25
26
27
28
29
30
31
32
33
34
35
36
37
38
39
40
41
42
43
44
45
46
47
48
49
50
51
52
53
54
55
56
57
58
59
60

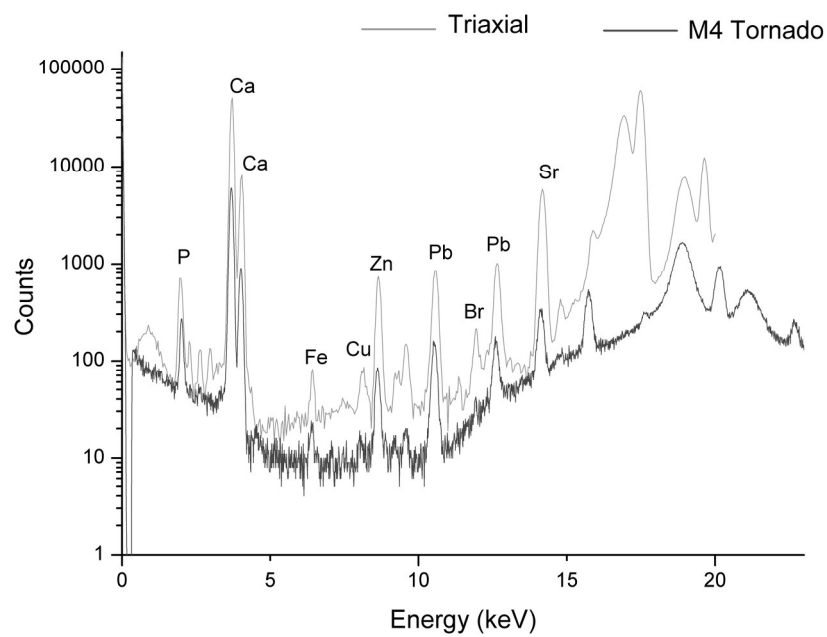


338x190mm (96 x 96 DPI)

1
2
3
4
5
6
7
8
9
10
11
12
13
14
15
16
17
18
19
20
21
22
23
24
25
26
27
28
29
30
31
32
33
34
35
36
37
38
39
40
41
42
43
44
45
46
47
48
49
50
51
52
53
54
55
56
57
58
59
60

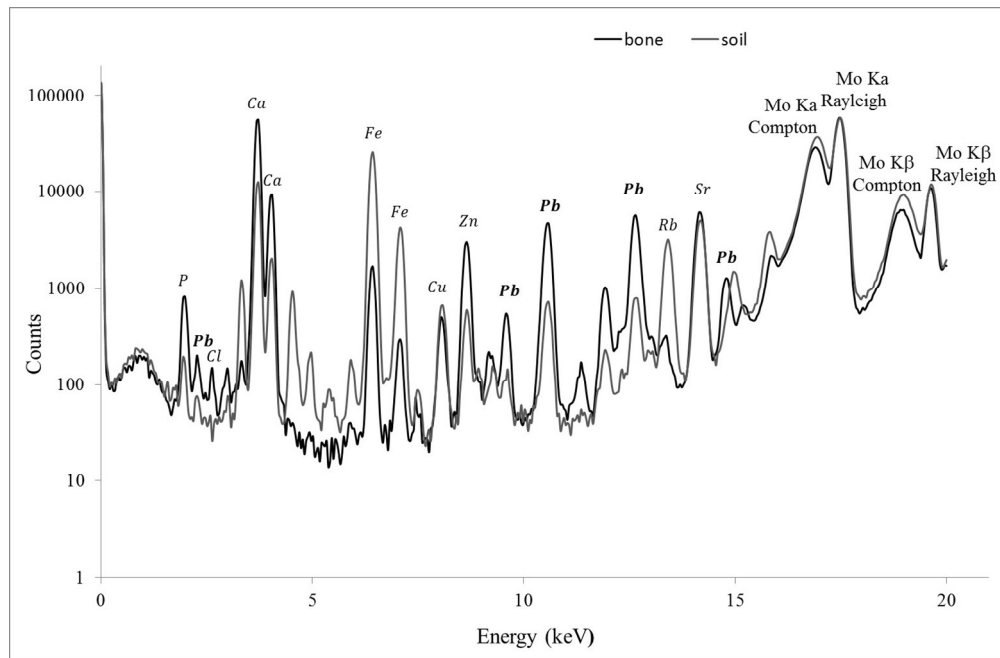


338x190mm (96 x 96 DPI)



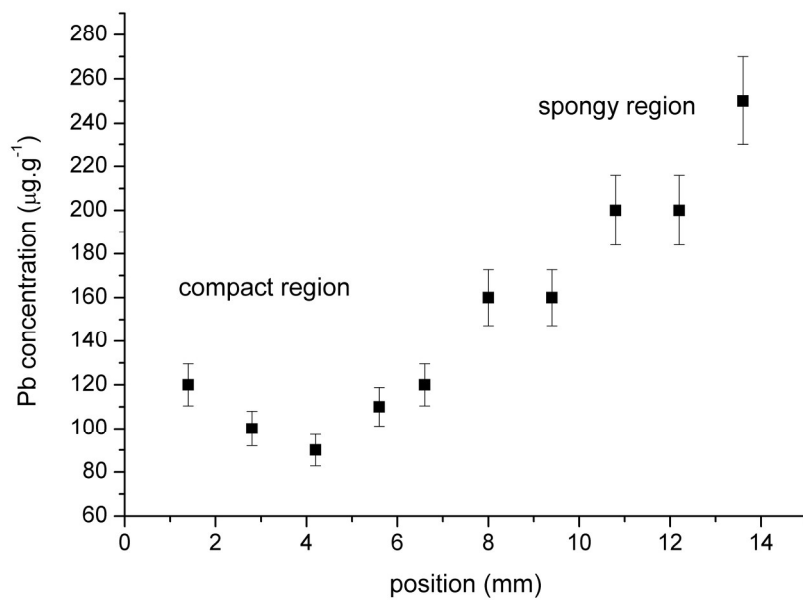
190x133mm (300 x 300 DPI)

1
2
3
4
5
6
7
8
9
10
11
12
13
14
15
16
17
18
19
20
21
22
23
24
25
26
27
28
29
30
31
32
33
34
35
36
37
38
39
40
41
42
43
44
45
46
47
48
49
50
51
52
53
54
55
56
57
58
59
60



291x190mm (133 x 133 DPI)

1
2
3
4
5
6
7
8
9
10
11
12
13
14
15
16
17
18
19
20
21
22
23
24
25
26
27
28
29
30
31
32
33
34
35
36
37
38
39
40
41
42
43
44
45
46
47
48
49
50
51
52
53
54
55
56
57
58
59
60



190x133mm (300 x 300 DPI)

Table 1. Accuracy and detection limits in $\mu\text{g g}^{-1}$ obtained for the the microanalytical system in bone samples (N= 4)

	NYS RM 05-02 Bovine Bone					NIST SRM 1400 Bone ash					NYS RM 05-04 Caprine Bone		
	Obtained triaxial setup	Obtained Tornado	Certified	Detection limits triaxial setup	Detection limits Tornado	Obtained triaxial setup	Obtained Tornado	Certified	Detection limits triaxial setup	Detection limits	Obtained triaxial setup	Obtained Tornado	Certified
Ca	27%±5%	30% ± 7%	26%	90	150	37% ± 1%	30% ± 7%	38.28% ± 0.13	100	150	27%±5%	29% ± 7%	26.4%
Zn	75±5	90 ± 20	80	2	30	180 ± 10	160 ± 30	181 ± 3	4	20	80±2	70 ± 10	81
Sr	150±10	170 ± 10	160	2	7	210 ± 20	240 ± 10	249 ± 7	3	7	155±5	150 ± 9	150
Pb	17±2	15 ± 9	16.1 ± 0.3	2	3	11 ± 3	7 ± 3	9.1 ± 0.1	3	3	33±3	30 ± 20	31.5 ± 0.7

Table 2. Accuracy and detection limits in $\mu\text{g g}^{-1}$ obtained for the microanalytical system in SRM IAEA-soil 7 samples (N= 4)

Element	Ca	Zn	Sr	Pb
Certified value	16.3% ± 6.0%	104 ± 3	108 ± 5	60 ± 5
Present work	16% ± 6%	110 ± 40	130 ± 50	50 ± 20
Detection limits	180	50	8	5

Table 3. Concentration values in, $\mu\text{g g}^{-1}$, for different bones obtained with microanalytical M4-Tornado system in pressed pellets (N=9)

Bones	Ca	Zn	Sr	Pb
Ribs	40% \pm 10%	600 \pm 100	220 \pm 30	600 \pm 90
Femur (spongy)	35% \pm 10%	1080 \pm 200	170 \pm 20	280 \pm 70
Skull	33% \pm 10%	196 \pm 34	160 \pm 20	220 \pm 50
Foot	34% \pm 10%	230 \pm 40	160 \pm 20	260 \pm 70
Fibula (comp)	40% \pm 10%	260 \pm 50	230 \pm 50	120 \pm 30
Fibula (spongy)	30% \pm 10%	80 \pm 20	150 \pm 30	250 \pm 50
Tibia (comp)	30% \pm 10%	110 \pm 20	170 \pm 40	100 \pm 25
Tibia (spongy)	39% \pm 10%	170 \pm 30	190 \pm 40	250 \pm 60

Table 4. Concentration values in, $\mu\text{g g}^{-1}$, for different bones obtained with triaxial system in pressed pellets (N=9)

Bones	Ca	Zn	Sr	Pb
Ribs	39% \pm 5%	500 \pm 30	210 \pm 10	560 \pm 30
Femur (spongy)	36% \pm 5%	980 \pm 50	200 \pm 10	300 \pm 20
Skull	32% \pm 5%	150 \pm 10	170 \pm 10	220 \pm 20
Foot	32% \pm 5%	170 \pm 10	180 \pm 10	300 \pm 20
Fibula (compact)	35% \pm 5%	220 \pm 20	210 \pm 10	190 \pm 20
Fibula (spongy)	37% \pm 5%	210 \pm 10	220 \pm 10	250 \pm 20
Tibia (compact)	37% \pm 5%	110 \pm 10	190 \pm 10	120 \pm 10
Tibia (spongy)	32% \pm 5%	140 \pm 10	220 \pm 20	260 \pm 20

Table 5. Concentration values in, $\mu\text{g g}^{-1}$, for different tooth region obtained with M4 Tornado for P, Ca, Zn, Sr and Pb in a tooth cross section (N=9)

Tooth					
	P	Ca	Zn	Sr	Pb
Enamel	19% \pm 5%	35% \pm 8%	110 \pm 22	100 \pm 6	16 \pm 9
Dentine	16% \pm 4%	31% \pm 7%	140 \pm 30	170 \pm 10	60 \pm 20
Root	16% \pm 4%	34% \pm 8%	190 \pm 30	190 \pm 10	130 \pm 50
Pulp	3% \pm 1%	4% \pm 1%	40 \pm 8	60 \pm 4	140 \pm 50